Neutron diffraction by germania, silica and radiation-damaged silica glasses

E. LORCH

Department of Physics (Applied Nuclear Science), University of Birmingham
MS. received 23rd August 1968

Abstract. Neutron diffraction patterns for vitreous germania, synthetic vitreous silica and radiation-damaged synthetic silica have been obtained to 18 Å^{-1}. With the use of a special resolution function the results have been analysed to produce 'radial distribution functions' free of truncation error ripples. The function for vitreous germania shows considerable improvement on previous x-ray measurements. Evidence for the concept of ordered groups of molecules in the glass is obtained from the radiation-damaged experiments.

1. Introduction

Synthetic vitreous silica is a glass produced by the vapour phase hydrolysis or oxidation of silicon compounds. Unlike the more orthodox glasses made by the fusing of crystalline forms of silica this glass does not go through an intermediate crystalline state (Lorch 1967) in its manufacturing process. Thus its structure would be similar but not necessarily identical to that of the fused quartz glasses.

Vitreous germania is a simple glass believed, as vitreous silica, to have tetrahedral co-ordination. Very little x-ray investigation of its structure is to be found in the literature (Zarzycki 1957) and no neutron diffraction results have been published.

The study of radiation-damaged glasses has been undertaken by several workers (Primak 1958, Simon 1957, Lukesh 1955) but information on the radial distribution functions and neutron diffraction patterns of such glasses seems also not to have been published.

2. Theory

The total differential coherent scattering cross section for neutrons (for a system of N particles) can be expressed in terms of the atomic density distribution, in the static approximation (Turchin 1965), as

$$\frac{d\sigma^{coh}}{d\Omega} = a_{coh}{}^2 \left[1 + \int_0^\infty \{g(r) - g_0\} \exp(-iQ \cdot r) \, dr \right] \tag{1}$$

where $g(r)$ is the atomic density distribution, g_0 is the mean atomic density, $\hbar Q$ is the momentum change of the neutron in the scatter process, and a_{coh} is the coherent scattering length. For a spherically symmetrical system with random orientation

$$\frac{d\sigma^{coh}}{d\Omega} = a^2 \left[1 + \int_0^\infty 4\pi r^2 \{g(r) - g_0\} \frac{\sin Qr}{Qr} \, dr \right]. \tag{2}$$

For a polyatomic system which can be divided into basic units (molecules) equation (2) becomes

$$\frac{d\sigma^{coh}}{d\Omega} = N_u \left[\sum_m a_m{}^2 + \sum_m a_m \sum_n a_n \int_0^\infty 4\pi r^2 \{g_{mn}(r) - g_{n0}\} \frac{\sin Qr}{Qr} \, dr \right] \tag{3}$$

where Σ_m is a summation over all the atoms (origins) in the basic unit, N_u is the number of such units, Σ_n is the sum over all the species of atoms in the system, $g_{mn}(r)$ is the atomic density distribution of n type atoms about the origin (m) atom and g_{n0} is the mean density

of type n atoms. Dividing equation (3) through by $N_u \Sigma a_m^2$ we have

$$i(Q) = \sum_m \sum_n \frac{a_n a_m}{\Sigma_m a_m^2} \int_0^\infty 4\pi r^2 \{g_{mn}(r) - g_{n0}\} \frac{\sin Qr}{Qr}\, dr \qquad (4)$$

and

$$i(Q) = \frac{1}{N_u} \frac{d\sigma^{coh}}{d\Omega} \frac{1}{\Sigma_m a_m^2} - 1.$$

$i(Q)$ is a normalized intensity obtained from the experimental diffraction pattern $I(Q)$:

$$i(Q) = \frac{I(Q) - I(\infty)}{I(\infty)} \qquad (4a)$$

where $I(\infty) = N_u \Sigma_m a_m^2$ and is the 'structure independent' coherent scattering obtained from the data at large momentum change (Q) values.

The Fourier transform of equation (4) is

$$\sum_m \sum_n a_m a_n 4\pi r^2 \{g_{mn}(r) - g_{n0}\} = \frac{2r}{\pi} \sum a_m^2 \int_0^\infty i(Q)\, Q \sin Qr\, dQ. \qquad (5)$$

If we write

$$\bar{g}(r) = \frac{\Sigma_m a_m \Sigma_n a_n g_{mn}(r)}{\Sigma_m a_m^2} \qquad (5a)$$

and

$$\bar{g}_0 = \frac{\Sigma_m a_m \Sigma_n a_n g_{n0}}{\Sigma_m a_m^2} \qquad (5b)$$

then equation (5) becomes

$$4\pi r^2 \{\bar{g}(r) - \bar{g}_0\} = \frac{2r}{\pi} \int_0^\infty Q i(Q) \sin Qr\, dQ. \qquad (6)$$

3. Truncation effect

For elastic scattering $Q = (4\pi/\lambda) \sin\theta$ where θ is half the scattering angle. In any experiment the range of Q values which can be covered is limited by instrumentally accessible values of λ and 2θ. This means that the experimental quantity $i(Q)$ can only be measured over a limited range of Q values which necessitates that the numerical solution of equation (6) be truncated at the maximum experimental value of Q, i.e. Q_{max}. This truncation leads to the appearance of spurious ripples in the radial distribution function and many workers (Furukawa 1962, Hosemann and Bagchi 1962) have dealt with their identification. However, the fact that results cannot be taken for momentum change values greater than some instrumentally determined maximum is equivalent to saying that the intensity of diffraction cannot be plotted for every point r in real space. If we say, however, that the scattering from a volume of space around r is the quantity detected, equation (6) may be written

$$\int_{r-\Delta/2}^{r+\Delta/2} 4\pi r^2 \{\bar{g}(r) - \bar{g}_0\}\, dr = \frac{2}{\pi} \int_{r-\Delta/2}^{r+\Delta/2} \int_0^{Q_{max}} Q i(Q) \sin Qr\, dQ\, r\, dr$$

where Δ is a small length in real space. If $\Delta \ll r$, $\{\bar{g}(r) - \bar{g}_0\}$ may be taken as constant over $r + \Delta/2$ to $r - \Delta/2$ and straightforward integration gives

$$4\pi r^2 \{\bar{g}(r) - \bar{g}_0\} = \frac{2r}{\pi} \int_0^{Q_{max}} i(Q) \frac{\sin Qr}{\Delta/2} \sin \frac{\Delta Q}{2}\, dQ \qquad (7)$$

where $\Delta = 2\pi/Q_{max}$ and Δ defines the resolution of the radial distribution function.

It is found that equation (7) removes spurious truncation ripples from the radial distribution function and allows more positive identification of the remaining maxima, some of which have been erroneously identified as truncation ripples by other workers.

4. Corrections to the normalized diffraction pattern

In the derivation of equation (1) (Turchin 1965) it is assumed that the scattered neutron loses an amount of energy small compared with its incident value. This is the so-called 'static approximation'. For neutrons of wavelengths of the order of 1 Å this approximation is in error. The error is partially compensated for by the use of the Placzek corrections (Turchin 1965, Plackzek 1952) and the form of these corrections for the polyatomic systems of equation (3) (Lorch 1967) is

$$\text{corrections} = -N_u \left[\sum_m a_m^2 \left\{ 1 - \frac{\alpha_m}{2E} \left(1 - \frac{1}{A_m} \right) + \frac{\bar{K}_m}{3E} \left(\frac{1}{A} - \frac{\alpha_m}{2E} \right) \right\} \right] \tag{8}$$

where $E = E_0/KT$, E_0 being the incident neutron energy, $\bar{K}$ is the average kinetic energy of the atom in units of KT, A is the mass ratio of scattering nucleus to neutron, and $\alpha = \hbar^2 Q^2 / 2MKT$, M being the mass of the scattering nucleus.

5. Vitreous germania

The diffraction pattern for vitreous germania was obtained using the twin-axis neutron spectrometer on the HERALD reactor at the Atomic Weapons Research Establishment, Aldermaston. The patterns were obtained in two stages using 1·18 Å neutrons to cover the region of momentum space from zero to 9·3 Å^{-1}, and 0·57 Å neutrons to extend the range from 9·3 Å^{-1} to 18 Å^{-1}.

An estimation for the multiple and incoherent backgrounds, which are assumed isotropic, is made by the usual technique of extrapolation to zero Q, figure 1. This extrapolation technique in no way affects the shape of the derived radial distribution function but enters directly when co-ordination numbers are calculated. The technique used for joining the two diffraction patterns differs from that of other workers and is explained further.
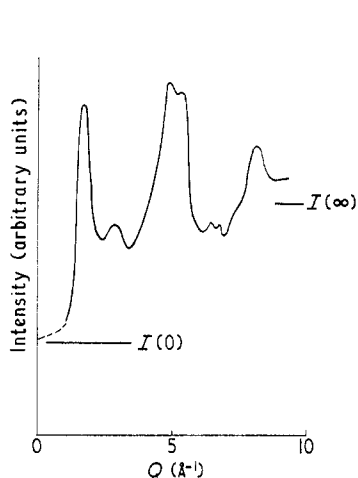

Figure 1. Neutron diffraction pattern of vitreous germania to 9·3 Å^{-1} obtained using 1·18 Å neutrons. The estimated values of the independent coherent scattering, $I(\infty)$ and the multiple plus incoherent scattering, $I(0)$, are also shown.
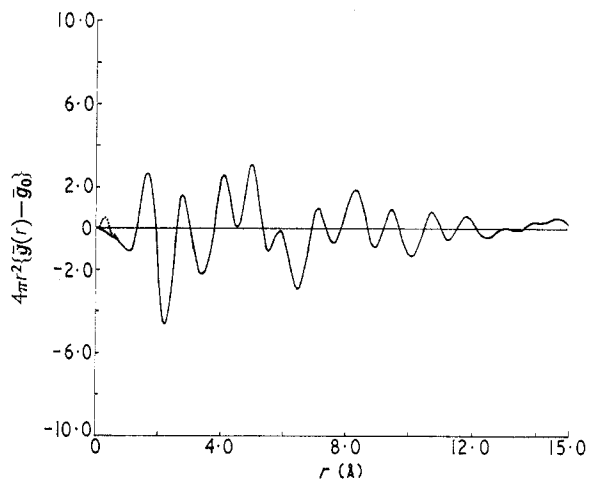
Figure 2. Radial distribution function for vitreous germania obtained from the Fourier transformation of the diffraction pattern of figure 1. The dotted curve shows the position of the ripple obtained when an incorrect value of $I(\infty)$ is used.

The Fourier transform of the data to $9 \cdot 3$ Å^{-1} has been performed using an estimated value of $I(\infty)$. The resulting low resolution radial distribution function is shown in figure 2. A small ripple is usually found at values of r less than the smallest interatomic spacing which is shown by the first major peak. From equation (6) and (4a) it is not difficult to show that an error $\Delta I(\infty)$ leads to an extra term ΔR in the radial distribution function (Lorch 1967) where

$$\Delta R(r) = \frac{-2\Delta I(\infty)}{\{I(\infty)+\Delta I(\infty)-I(0)\}} \frac{\sin rQ_{max}}{r} \left\{1 - \left(\frac{\pi}{Q_{max}}\right)^2 \frac{1}{r^2}\right\}^{-1} \tag{9}$$

that is a damped periodic function which, if $\Delta I(\infty) \ll I(\infty)$, is proportional to $\Delta I(\infty)$. A plot of ripple amplitude against estimated $I(\infty)$ produces the curve of figure 3 from which
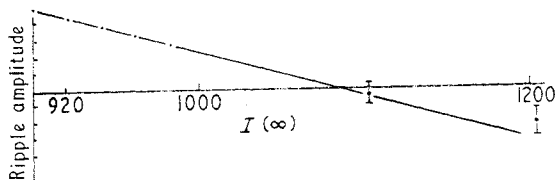

Figure 3. Ripple amplitude against estimated value of $I(\infty)$. The $I(\infty)$ intercept gives the value used in the Fourier transformation.
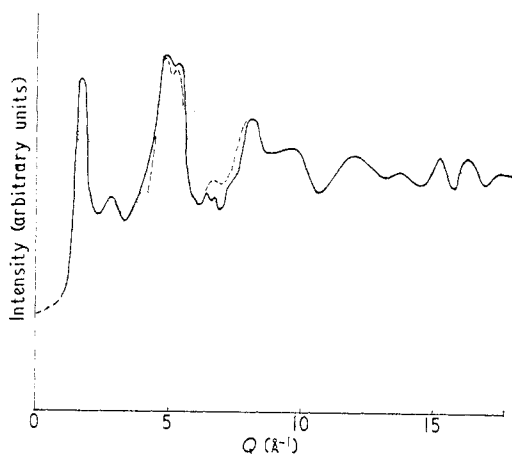

Figure 4. Mated diffraction pattern of vitreous germania; the broken curve shows the value of the $0 \cdot 57$ Å pattern in the region of overlap.
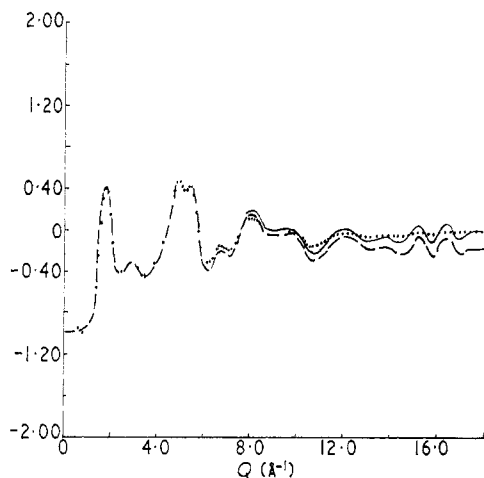
Figure 5. Normalized diffraction pattern for vitreous germania showing the effect of the Placzek corrections: – – – – – normalized incident pattern; ———— normalized incident pattern with Placzek corrections; ... pattern obtained by reverse Fourier transformation of the radial distribution function.

the value of $I(\infty)$ is estimated. The $0 \cdot 57$ Å pattern was then normalized at 8 Å^{-1} to the value of the $1 \cdot 18$ Å pattern at the same peak. The resulting diffraction pattern with a common overlap region is shown in figure 4. The normalized diffraction pattern corresponding to equation (4a) is given in figure 5. The general tendency for the distribution to curve downwards with increasing Q as predicted by the Placzek corrections is clearly observed. For vitreous germania the corrections are evaluated as

$$C = -3 \cdot 65 \times 10^{-4} Q^2 + 4 \cdot 1 \times 10^{-3}.$$

Application of this correction causes the pattern to return to a function oscillating around zero, figure 5, showing that the zero-ripple value of $I(\infty)$ is a good fit for the normalization procedure.

The Fourier transforms of the corrected and uncorrected patterns have been performed using increments (Ino 1957) of Q of $0 \cdot 1 \text{ Å}^{-1}$ in the numerical integration of equation (7). Differences between the two radial distribution functions are found to be confined to the magnitude of the ripples before the first major peak (figure 6). Use of the corrections
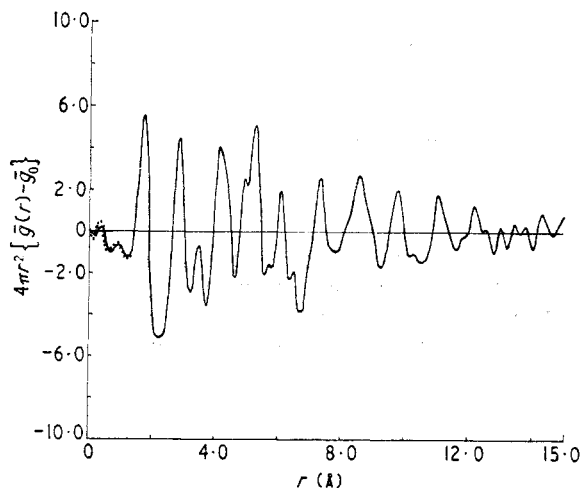

Figure 6. Radial distribution function from 18 Å^{-1} mated diffraction pattern of vitreous germania (figure 4) showing position of spurious ripples and effect of Placzek corrections: ——— Placzek corrected pattern; .... uncorrected pattern.
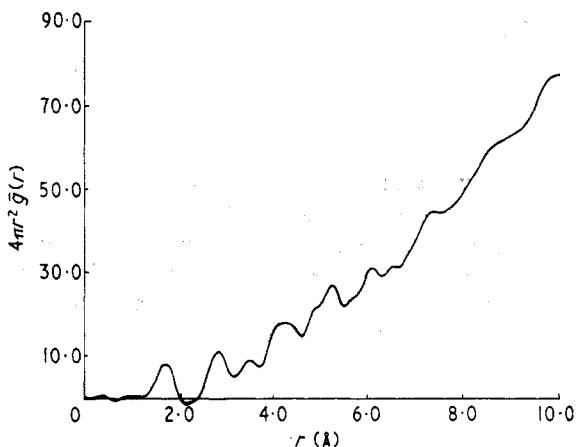
Figure 7. Total radial distribution function of vitreous germania.

causes a reduction of up to 50% in their amplitude. In general the resulting radial distribution functions are not found to be very sensitive to the detail of the tail owing to the dampening effect on $i(Q)$ of the $\sin \Delta Q/2$ term of equation (7). This is clearly shown by the dotted curve of figure 5 which is the reverse Fourier transform of the radial distribution function corresponding to the uncorrected diffraction pattern. This shows that when equation (7) is used the corrections may generally be neglected if no importance is attached to the ripples at small distances. The differential and total radial distribution functions are shown in figures 6 and 7 and comparison of the results with those of Zarzycki (1957) using x-rays shows the improvement in radial distribution function resolution. Major peaks are found in the total radial distribution function at the position indicated in table 1.

Crystalline germania is known to exist in two phases; the first with α-quartz type structure having tetrahedrally co-ordinated germania and the second a rutile structure having octahedral co-ordination. The densities of these two phases are $4 \cdot 2 \text{ g cm}^{-3}$ and $6 \cdot 2 \text{ g cm}^{-3}$ respectively whereas that for germania glass is $3 \cdot 65 \text{ g cm}^{-3}$. The densities alone provide some indication of the type of co-ordination present. The co-ordination number for germania glass is calculated from the area of the first peak in the radial distribution function as $3 \cdot 8$ in reasonable agreement with that expected for tetrahedral co-ordination, namely 4. Estimation of co-ordination numbers is, however, necessarily approximate owing to the extrapolation method used to estimate $I(0)$ for the multiple and incoherent contribution, a quantity which enters directly into the calculation of the radial distribution function. It is to be noted that in this particular case it would be impossible to obtain a higher co-ordination number without *upward* extrapolation of the curve at low Q values.

Table 1. Position of peaks in total radial distribution function of germania glass

Peak	Position (Å)	Identification
1	1·72	Ge–O
2	2·85	O–O
3	3·45	Ge–Ge
4	4·2	Ge–2O[a]
5	4·9	O–2O[a]
6	5·27	Ge–2Ge[a]
7	6·05	

[a] These peaks are not due to one type of co-ordination and should not be rigorously interpreted.

6. Synthetic vitreous silica

The sample was studied in a two-wavelength experiment identical to that used for vitreous germania. The corrected normalized mated diffraction pattern is shown in figure 8 and corresponding total radial distribution function in figure 9. Clear detail is seen out to at least 6 Å, the first two peaks being identified as the Si–O and O–O co-ordination respectively.
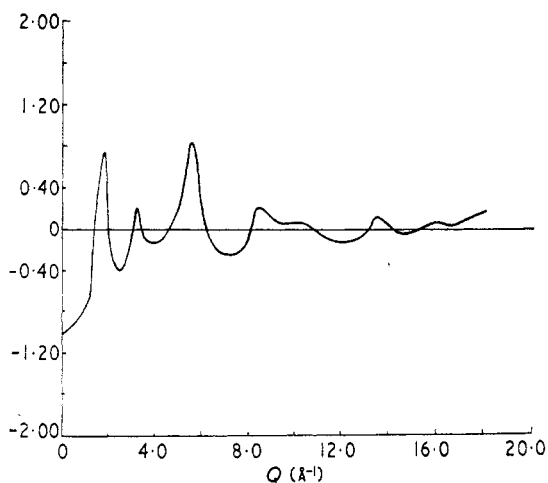

Figure 8. Normalized diffraction pattern of synthetic vitreous silica.
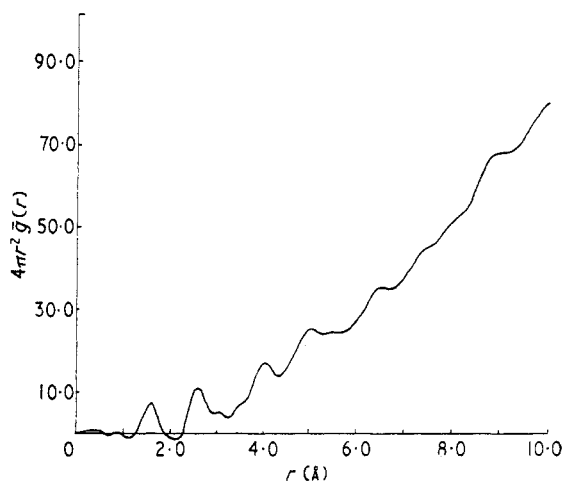

Figure 9. Total radial distribution function of synthetic vitreous silica.

Table 2. Main peaks in radial distribution functions of silica and radiation-damaged silica glasses

	Distances (Å)			
	Silica glasses			Radiation-damaged glass
Possible atomic pair	Present work	Heaton (1967) (neutron)	Robinson (1965)[†] (x-ray)	Present work
Si–O	1·60 ±0·05	1·59	1·62	1·6 ±0·05
O–O	2·6	2·62	2·62	2·6
Si–Si	3·05	3·22	3·05	3·05
Si–2O	3·60	3·7		3·55
O–2O	4·05	4·09	4·08	3·95
	5·02	5·03	5·02	5·1

[†] Refers to work by Norman.

A summary of the peaks is given in table 2 together with those of several other workers. Attention is drawn to the appearance of a peak at about 3·6 Å which has also been detected by other workers (Heaton 1967, Carraro 1965) but has often been identified as a truncation ripple. Its appearance here, in spite of use of the resolution function (equation (7)) strongly suggests that it has a structural origin and it will be significant in any comparison made between the vitreous radial distribution function and the statistics of co-ordination of the various forms of crystalline silica.

7. Radiation-damaged Spectrosil

A Spectrosil sample cut from the same block as that for which the above results were given was exposed to an estimated fast neutron flux of $2·04 \times 10^{20}$ n.v.t. The density of the irradiated sample was 2·254 g cm^{-3} showing a 2·6% increase on that of the control specimen. The specimen was found to have acquired a deep blue colour whereas the control was colourless. The corrected normalized neutron diffraction pattern of figure 10 was obtained in the manner described for the previous two samples. The Fourier transform is given in
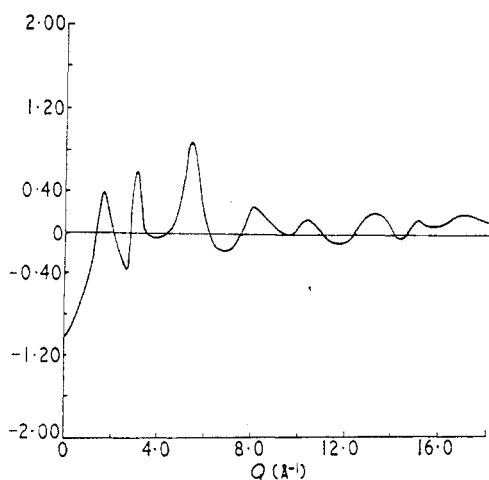

Figure 10. Normalized diffraction pattern of radiation-damaged synthetic vitreous silica.
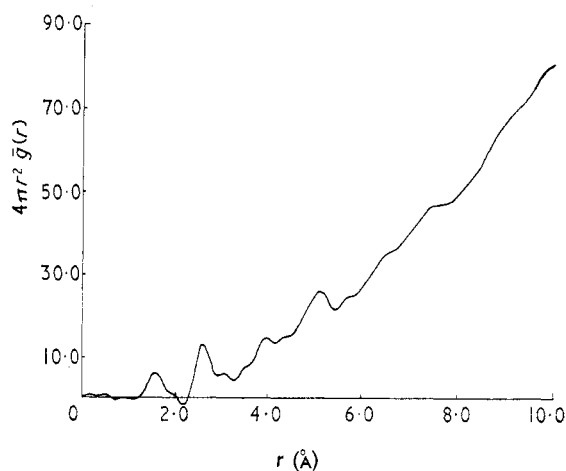

Figure 11. Total radial distribution function for radiation-damaged synthetic vitreous silica.

figure 11 and the listing of the peaks in table 2. Because of the magnitude of the experimental error no significance can be given to the fact that peaks 4 and 5 lie at smaller distances than for the control specimen. Detail after the 5·1 Å maxima is very weak suggesting that ordered structure does not extend greatly beyond this limit. The areas under all the maxima show a decrease with the Si–O peak showing the greatest change. The change in shape of the first peak is also noted, the subsequent 'hump' suggesting a preferential site for the displaced atoms. It may be significant that all the major peaks appear to be followed by such a 'hump'. Of still more importance, from the author's point of view, are the changes which have occurred in the diffraction pattern on irradiation. The clearest of these is the drastic reduction in the area of the first peak. Comparison of figure 10 with figure 8 shows that this peak has decreased perhaps 20% in area. It seems reasonable to postulate that the normal diffraction pattern is constructed from two portions, the low Q portion showing co-ordination of some extra molecular unit, perhaps rings, whereas the higher subsequent Q portion reflects the internal molecular structure. Such extra molecular units will have their own scattering centres defined by an equation of the form

$$N(a_{Si} + 2a_O)R_m = a_{Si}R_1 + a_O R_2 + a_O R_3 + \ldots a_{Si}R_n + a_O R_{n+1} + \ldots$$

where R_m is the vector position of the scattering centre, R_n is the vector position of the nth atom in the unit, N is the number of molecules in the unit, a_{Si} is the neutron scattering length of the Si atoms, and a_O is the neutron scattering length of the O atoms.

Obviously displacement of a few of the atoms will lead to a redefinition of R_m and the unit's scattering centre will lose its correlation with respect to the other units. This is reflected in the decrease in the area of the first diffraction peak. However, whereas displacement of even a single atom leads theoretically to a redefinition of R_m the effect on the internal correlation of the N molecules will be small, displacement of one atom affecting at the most the internal correlation of two silica tetrahedra. The above argument simply reasons that there is a reduction in the long-range order of the glass but it is useful in that it introduces the idea of clusters of tetrahedra. As a further illustration of this effect the Fourier transform of the diffraction pattern to 4 Å^{-1} has been performed. This process is meaningful owing to the use of the resolution function which ensures that the radial distribution function corresponds to that part of the diffraction pattern which dampens out by 4 Å^{-1} and effectively rejects overlapping information from high Q portions of the pattern, compare with the overlapping of two Gaussians. The radial distribution function so obtained is shown in figure 12 and it is clearly seen that no information is present for
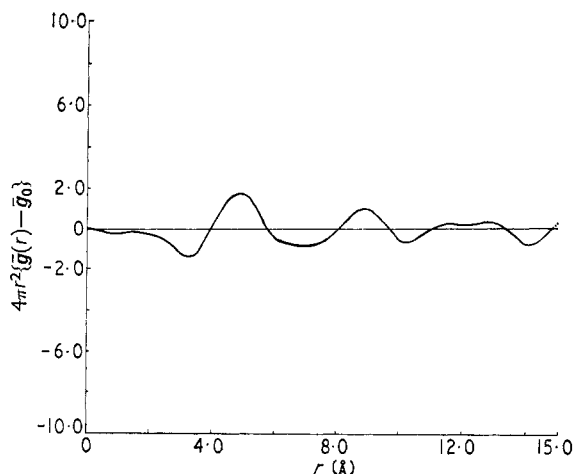

Figure 12. Radial distribution function obtained from Fourier transforming vitreous silica pattern to $Q_{\max} = 4 \text{ Å}^{-1}$.

distances corresponding to those of the internal dimensions of the basic tetrahedra, i.e. $2 \cdot 65 \text{ Å}$. At this stage the first broad peak at approximately $4 \cdot 9 \text{ Å}$ is taken to show the scattering centre corresponding to some grouping, possibly rings, of tetrahedra. A simple calculation on a perfect six-sided ring gives a 'diameter' of $5 \cdot 3 \text{ Å}$. In any true model of the glass many different types of rings are to be expected with a possible preference for five-sided grouping (Oberlies and Dietzel 1957) and a resulting smaller diameter.

8. Conclusion

Although the origin of spurious ripples in the radial distribution functions has been investigated and possible causes found it has not been possible to eliminate them completely. The ripples before the first major peak, which represent the smallest interatomic distance, are very sensitive to the value of the term $I(\infty)$ of equation (4a) and are not structurally significant. No other peaks in the radial distribution function show the same sensitivity to $I(\infty)$.

New data have been presented for vitreous germania and radiation-damaged vitreous silica and the radial distribution function for synthetic vitreous silica has been found to be basically the same as that for ordinary vitreous silica.

Finally it should be noted that in any more detailed analysis of radial distribution functions consideration must be given to the effect of distortions inherent in diffraction patterns obtained by the standard method of twin-axis neutron spectroscopy. These distortions are due to deviations from the static approximation (Placzek 1952, Turchin 1965) and are only partly compensated for by the correction given by equation (8).

Acknowledgments

References

CARRARO, G., 1965, *Physics of Non-Crystalline Solids*, Ed. J. A. Prins (Amsterdam: North Holland).

FURUKAWA, G., 1962, *Rep. Prog. Phys.*, **25**, 396–435 (London Institute of Physics and Physical Society).

HEATON, L., 1967, *J. Phys. Chem. Solids*, **28**, 423–32.

HOSEMANN, R., and BAGCHI, S. N., 1962, *Direct Analysis of Diffraction by Matter* (Amsterdam: North Holland).

INO, T., 1957, *J. Phys. Soc. Japan*, **12**, 495–506.

LORCH, E., 1967, *Ph. D. Thesis*, University of Birmingham.

LUKESH, J., 1955, *Phys. Rev.*, **97**, 345–6.

OBERLIES, F., and DIETZEL, A., 1957, *Glastech. Ber.*, **30**, 37–42.

PLACZEK, G., 1952, *Phys. Rev.*, **86**, 377–88.

PRIMAK, W., 1958, *Phys. Rev.*, **110**, 1240–54.

ROBINSON, H., 1965, *J. Phys. Chem. Solids*, **26**, 214.

SIMON, I., 1957, *J. Am. Ceram. Soc.*, **40**, 150–4.

TURCHIN, V., 1965, *Slow Neutrons*, Israel Program for Scientific Translations, p. 104.

ZARZYCKI, J., 1957, *Verres Réfract.*, **11**, 3–8.